RSC Advances

Accepted Manuscript

This article can be cited before page numbers have been issued, to do this please use: V. Shinde and G. Madras, *RSC Adv.*, 2013, DOI: 10.1039/C3RA45961F.

View Article Online
DOI: 10.1039/C3RA45961F

Catalytic performance of highly dispersed Ni/TiO_2 for dry and steam reforming of methane

Vijay M. Shinde, Giridhar Madras[*]

Department of Chemical Engineering,

Indian Institute of Science, Bangalore-560 012. INDIA

[*]Corresponding author Tel.: +91-80-22932321; Fax: +91-80-23601310.

E-mail: giridhar@chemeng.iisc.ernet.in

View Article Online
DOI: 10.1039/C3RA45961F

Abstract

The present study reports a sonochemical assisted synthesis of highly active and coke resistant Ni/TiO_2 catalyst for dry and steam reforming of methane. The catalyst was characterized using XRD, TEM, XPS, BET analyzer and TGA/DTA techniques. TEM analysis showed that Ni nanoparticles were uniformly dispersed on TiO_2 surface with a narrow size distribution. The catalyst prepared via this approach exhibited excellent activity and stability for both the reactions than the reference catalyst prepared from the conventional wet impregnation method. For dry reforming, 86% CH_4 conversion and 84% CO_2 conversion was obtained at 700°C. Nearly 92% CH_4 conversion and 77% CO selectivity was observed under H_2O/CH_4 ratio of 1.2 at 700°C for the steam reforming reaction. In particular, the present catalyst is extremely active and resistant to coke formation for steam reforming at low steam/carbon ratio. There is no significant modification of Ni particles size and no coke deposition, even after long term reaction, demonstrating its potential applicability in industrial reformate for hydrogen production. The detailed kinetic studies have been presented for steam reforming and the mechanism involving Langmuir-Hinshelwood kinetics with adsorptive dissociation of CH_4 as a rate determining step has been used to correlate the experimental data.

Keywords: dry reforming; steam reforming; hydrogen production; coke deposition; nickel catalyst.

View Article Online
DOI: 10.1039/C3RA45961F

1. Introduction

The steam reforming of methane is a well established industrial process for the production of hydrogen and synthetic gas[1,2]. Ni based catalysts are commonly used in industrial reforming reaction due to their low cost and reasonably good activity. However, these catalysts deactivate due to sintering and coke deposition.[3] Therefore, excess steam (H_2O/CH_4>3) is introduced in the feedstock to prevent coke deposition. Though excess steam favors higher conversion, unnecessary generation of steam hampers the process economy and increases the H_2/CO ratio. This make the stream unsuitable for downstream processes such as Fischer-Tropsch synthesis.[4] Further, it increases the size of reactor and the required amount of catalyst. It also leads to deactivation of the catalyst due to oxidation of Ni particle.[5] Therefore, the inhibition of coke deposition under low H_2O/CH_4 ratio on the Ni-based catalysts is one of the biggest challenges in the steam reforming process.

Several studies discuss enhancing the stability of Ni based catalysts for the reforming reaction. Promoters such as alkaline earth oxide (MgO or CaO) are often used to lower the coking propensity and provide higher stability against sintering.[6, 7] However, the addition of these promoters impedes the reduction of NiO leading to the decrease in the activity. It has been observed that the promotion with K or Ca increase the formation of $NiAl_2O_4$ phase, which is reducible above 700°C.[8] Horiuchi et al. reported that the addition of alkaline metal suppressed the reforming activity of Ni with the markedly suppression of coke deposition for dry reforming reaction.[7] Therefore, it is better to modify Ni-based catalysts without compromising their activity.

It is evident that the reducible supports (CeO_2, TiO_2) provide better stability and coke resistance in comparison with their non-reducible supports counterparts (Al_2O_3, SiO_2).[9-11] There

View Article Online
DOI: 10.1039/C3RA45961F

is a direct correlation between oxygen storage capacity (OSC) and coke deposition propensity: higher the OSC, lower is the coke deposition on the catalyst.[12] Ceria and modified ceria compounds are well known for their reversible exchange of lattice oxygen during the reaction.[13-15] However, CeO_2 support is vulnerable to sintering and loses its OSC at high temperature.[16] TiO_2 exhibits lower OSC compared to CeO_2 but is stable at high temperature. The dry reforming was studied over Ni supported on various supports and specific activities followed the order: $Ni/TiO_2 > Ni/C > Ni/SiO_2 > Ni/MgO$.[17] Therefore, TiO_2 seems to be good alternative support for CeO_2 and Al_2O_3.

The activity of the catalyst often depends on the size and extent of metal dispersion.[18, 19] Small particles increases metal dispersion and also provides more steps/kinks on the surface.[20, 21] The energy barrier for methane dissociation, a rate determining step, over step sites is much lower than stair sites. Therefore, the rate of reaction increases with the extent of dispersion of active phase.[22, 23] Further, small particles below a critical size have also been reported to be more resistant to coke formation and the spillover of steam on the support is a key parameter between particle size and rate of coke deposition.[20, 24] The highly dispersed metal particles also tend to minimize surface energy by increasing interaction with the support and hence minimizing sintering.[22] Therefore, the synthesis of homogeneous and highly dispersed Ni nanosized particles with a significant metal support interaction is essential for stable performance.

The preparation method often influences structure and morphology of the catalyst. Recently, it was shown that a sonochemical assisted method produces uniformly dispersed nanoparticles with a narrow size distribution in range of 8-9 nm.[25, 26] Here, we report a sonochemical assisted synthesis of highly active and coke resistant Ni/TiO_2 catalyst for dry and steam reforming of methane. In contrast to the conventional wet impregnation method, the metal

View Article Online
DOI: 10.1039/C3RA45961F

precursor of active phase and support are added together to an aqueous solution and irradiated using high intensity ultrasonic horn resulting in a very fine dispersion of active phase. The catalytic performance of the material was investigated by performing dry and steam reforming reactions. High activity and stability was manifested for both the reactions. The intrinsic kinetics over a wide range of temperature was studied for the steam reforming reaction and the effect of inlet concentration of reactants and products on rate of reaction was investigated. A Langmuir-Hinshelwood mechanism was used to correlate the experimental data.

2. Experimental

2.1Synthesis and characterization

Titanyl nitrate ($TiO(NO_3)_2$) solution, and nickel nitrate (S.D Fine, India) were used as starting materials for the synthesis of 15 % Ni/TiO_2. A white colored $TiO(OH)_2$ was precipitated by the controlled hydrolysis of 5 ml of titanium isopropoxide (Alfa Aesar, India) under ice cold (4°C). 10 ml HNO_3 was added to obtain a clear solution of $TiO(NO_3)_2$. In another precursor solution, 0.99 g of nickel nitrate was dissolved in 20 ml of distilled water and both the solutions were mixed together. The resulting solution was sonicated for 3 h using a high intensity Ti-horn probe of 25 mm diameter (50 KHz, and 125 W/cm^2 at 60% efficiency). The powder was separated, washed with water-ethanol mixture, and dried in hot air oven at 120°C. The catalytic activity of 15% Ni/TiO_2 catalyst, synthesized by conventional wet impregnation method was synthesized and compared with the catalyst synthesized via sonication method. For this purpose, pure known weight of TiO_2 (prepared by sonication method) was dispersed in water and nickel nitrate equivalent to 15 wt % was added. Ni^{2+} ions were reduced to Ni metals by hydrazine hydrate (S.D Fine, India) solution at room temperature. The solid was separated and dried at 120° C. Both the powders were further calcined at 700° C for 1 h. The catalyst synthesized via

View Article Online
DOI: 10.1039/C3RA45961F

sonochemical method is designated as 15% Ni/TiO_2 (sonic) while the catalyst synthesized via impregnation method is designated as 15% Ni/TiO_2 (imp).

X-ray diffraction (XRD) patterns were recorded on a Philips X'Pert diffractometer with Cu-Kα radiation (λ=1.54178 Å) in the 2θ range of 20-80°. Transmission electron microscopy (TEM; FEI Technai 20) was used to study morphology and microstructures of the catalyst. The TEM specimen was prepared by dropping a trace amount of sample dispersed in ethanol on a carbon coated grid (300 mesh). XPS spectra were recorded on a Thermo Scientific Multilab 2000 instrument with monochromatized Al-Kα X-rays (1486.6 eV). The binding energies were charge corrected using the C 1s peak observed at 285 eV. The BET area measurement was carried out with a Quantachrome NOVA 1000 gas adsorption analyzer. Prior to the measurement, the sample was degassed at 150°C for 4 h under vacuum. The amount of carbon deposited during long term stability test was determined using thermo-gravimetric analysis and differential thermal analysis (TGA/DTA). The experiment was performed on a Mettler Toledo thermal analyzer under O_2 flow of 30 ml/min with a heating rate of 10° C/min.

2.2 Catalytic studies

Dry reforming of CH_4 was studied in a fixed bed reactor under atmospheric pressure. The quartz reactor (4 mm ID and length of 30 cm) was heated in an electric furnace and the temperature of bed was controlled by a K-type thermocouple positioned in the center of the catalyst bed. 75 mg of catalyst was packed between two glass wool plugs in the center of reactor. The feed mixture consisting of 2 % CH_4, 2 % CO_2 and balance of N_2 keeping the total flow rate at 100 ml/min (GHSV of 95500 h^{-1} is based on the catalyst bed volume of 0.0628 cm^3). The oxidized catalyst in air showed the formation of inactive $NiTiO_3$ phase and no activity for both the reactions. Therefore, the catalyst was reduced at 650°C for 2 h with pure H_2 at a flow of 20

View Article Online
DOI: 10.1039/C3RA45961F

ml/min before the reaction. The product was analyzed using an on-line gas chromatograph (Mayura Analytical Bangalore, India) equipped with a TCD and FID (incorporating a methanator). The conversions (X) and the H_2/CO ratio were calculated as follows

$$X_{CH_4}(\%) = \frac{[CH_4]_{in} - [CH_4]_{out}}{[CH_4]_{in}} \times 100 \quad (1)$$

$$X_{CO_2}(\%) = \frac{[CO_2]_{in} - [CO_2]_{out}}{[CO_2]_{in}} \times 100 \quad (2)$$

$$\frac{H_2}{CO}\, ratio = \frac{mol\ of\ H_2 produced}{mol\ of\ \mathrm{CO}\ produced} \quad (3)$$

The bracketed quantity represents the concentration of the component in the product stream. The activity of the catalyst was measured under steady state at various temperatures. In order to ensure steady state, the temperature of the reactor was set at desired value and the gases were allowed to flow over the catalyst continuously. After 15 min, four readings at the same temperature were averaged. The temperature of the reactor was then set to the next high temperature and the same procedure was repeated. The average of the four readings was taken for the calculation and standard deviation of reported conversion was less than 3%. The experimental data was collected under the absence of any external and internal diffusion limitation.

The steam reforming reaction was carried over 150 mg of catalyst diluted by required amount of glass beads. The feed mixture consisting of 3 vol % of CH_4 and balance of N_2 was passed at rate of 100 ml/min. This corresponds to the gas hourly space velocity of 48000 h^{-1} (based on the catalyst bed volume of 0.125 cm^3). Water was fed to the steam generator using a HPLC pump (Waters 515) at flow rate of 0.1 ml/min and the generated vapor (3.6 ml/min) was mixed with reaction mixture before entering the reactor. A moisture trap was kept at the outlet of

View Article Online
DOI: 10.1039/C3RA45961F

the reactor to condense any water from the product gas stream. Prior to reaction, the catalyst was reduced in pure H_2 with a flow rate of 20 ml/min for 2 h at 650°C. The CH_4 conversion (X) and CO selectivity were calculated as follows

$$X_{CH_4}(\%) = \frac{[CO]+[CO_2]}{[CO]+[CO_2]+[CH_4]} \times 100 \quad (4)$$

$$CO\ selectivity\ (\%) = \frac{[CO]}{[CO]+[CO_2]} \times 100 \quad (5)$$

The rate of formation of (CO + CO_2) was nearly same to the rate of disappearance of CH_4 which indicates that the rate of carbon formation was negligible over the catalyst.

3. Results and discussion

3.1. Structural studies

XRD patterns of both the catalysts before and after the steam reforming reaction are shown in Fig.1. 15% Ni/TiO_2 (sonic) catalyst shows well resolved peaks characteristic of a rutile structure of TiO_2. The peaks observed at 2θ = 76.4, 51.8 and 44.5° can be assigned to the (220), (200), (111) planes of Ni metal, respectively. However, 15% Ni/TiO_2 (imp) catalyst shows peaks due to metallic Ni (111) along with anatase phases of TiO_2. The small peak at 27.4° indicates that the small amount of rutile phase is also present in 15% Ni/TiO_2 (imp) catalyst. The average crystallite size of Ni was determined by the peak broadening of the (111) reflection in the XRD patterns, using the Scherrer formula and was found to be 13 nm and 19 nm respectively, for 15% Ni/TiO_2 (sonic) and 15% Ni/TiO_2 (imp) catalyst. Further, the close observation of XRD patterns of 15% Ni/TiO_2 (sonic) catalyst shows that the peak of rutile TiO_2 phase observed at 27.6° is shifted to higher values by 0.4° due to decrease in d-spacing. This shows partial substitution of Ni into TiO_2 lattice during synthesis. In contrast, no shift in XRD pattern of 15% Ni/TiO_2 (imp)

View Article Online
DOI: 10.1039/C3RA45961F

catalyst was observed. Therefore, partial incorporation of Ni into TiO_2 lattice is possible during synthesis.

It is well known that Ni/TiO_2 catalyst deactivates due to the formation of $NiTiO_3$ phase and oxidation of Ni species, which make the catalyst more difficult to reduce during the reaction. Therefore, the XRD patterns were also recorded after the reaction to observe the changes in the catalyst structure. The XRD patterns of 15% Ni/TiO_2 (sonic) shows that the rutile structure of TiO_2 was retained after the reaction and reflections either due to NiO or $NiTiO_3$ were not observed indicating catalyst is stable and not oxidized during the reaction. For Ni/TiO_2 (imp) catalyst, peaks either due to NiO or $NiTiO_3$ is also absent. However, the formation of the rutile phase was found to be high after the reaction.

Bright field images of 15% Ni/TiO_2 (sonic) and 15% Ni/TiO_2 (imp) catalyst are shown in Fig. 2. In the as synthesized 15% Ni/TiO_2 (sonic) catalyst (Fig 2a), Ni particles are spherical and uniformly distributed over TiO_2 support and no aggregation of particles was observed. The average particle size of Ni species was 8-10 nm. After calcination at 700°C, the size of Ni nanoparticles slightly increased. The average particle size of Ni is about 14-16 nm, which is similar to the size calculated from the broadening of XRD diffraction patterns. After 16 h of steady state test reaction, the presence of appreciable carbon was not observed (Fig. 2c), which is an agreement with TGA/DTA (~0.6 wt %) results. The TEM image shows that Ni particles retained physical contact with TiO_2 support and no considerable agglomeration of Ni species was observed. However, the average particle size Ni metal is between 16-18 nm. This shows that there is no appreciable increase in the size of Ni particles (compared to calcinated catalyst) during the reaction. In contrast, 15% Ni/TiO_2 (imp) catalyst form large nanoparticles compared to 15% Ni/TiO_2 (sonic) catalyst (Fig. 2d). The BET surface area for the catalyst before and after

View Article Online
DOI: 10.1039/C3RA45961F

the steam reforming reaction was found to be 62 and 49 m^2/ g, respectively. This reduction in surface areas may be due to an increase in particles size.

Fig.3 shows XPS of both the catalysts. The NiO species is characterized by the peak at binding energy of 854.6 eV along with the broad satellite at around 860 eV.[27] A peak at binding energy of 852.6 eV corresponds to Ni^0 metal.[28] The main Ni (2p) peak was deconvoluted corresponding to the Ni^{2+} and Ni^0 states. Ti ($2p_{3/2}$) binding energies are observed at ~ 458.9 eV in both the catalysts is correspond to a Ti ion in the +4 state.[29] The spectra of the spent catalyst were very broad, indicating the partial reduction of Ti^{4+} ions to the Ti^{3+} state. The Ti^{3+} ion in Ti_2O_3 is observed at 458.2 eV.[29] It was found that the binding energy of Ni (2p) and Ti (2p) peaks in 15% Ni/TiO_2 (sonic) catalyst were shifted slightly to higher value compared to 15% Ni/TiO_2 (imp) catalyst. The shift in binding energy of Ni (2p) in 15% Ni/TiO_2 (sonic) catalyst is due to the different chemical environment of the substituted Ni ions in the catalyst compared to that of the pure Ni ions in NiO. The metal-support interaction has previously been observed after steam treatment of Ni/Al_2O_3 catalyst and a shift in binding energy of Ni 2p and Al 2p peaks towards higher value was observed after steam pretreatment.[30] The surface concentration of Ni in both the catalysts was estimated from the intensities of Ni (2p) and Ti (2p) peak. The relative surface concentration was calculated from

$$\text{Concentration, } C_M = \frac{I_M / (\lambda_M \sigma_M D_M)}{\sum (I_M / (\lambda_M \sigma_M D_M))} \quad (6)$$

I_M, λ_M, σ_M and D_M is the integral intensity of Ni (2p) and Ti (2p) peak, mean escape depths of the respective photoelectrons, photoionization cross section and geometric factor, respectively. The photoionization cross-section values and mean escape depths were taken from the literature.[31, 32] The geometric factor was taken as 1, since the maximum intensity in this spectrometer is obtained at 90°. The relative surface concentration of Ni species obtained for 15% Ni/TiO_2

View Article Online
DOI: 10.1039/C3RA45961F

(sonic) and 15% Ni/TiO_2 (ionic) was 26 % and 19% at, respectively, which is much higher than 15 wt % (15 wt % corresponds to 17% at) taken in the preparation. After the reaction, the relative surface concentration of Ni species for 15% Ni/TiO_2 (sonic) catalyst was found to be 18%.

3.2 Catalytic performance for dry reforming

The activity of the catalyst for the dry reforming was expressed in terms of conversion of reactants. The variation of CH_4 and CO_2 conversions over 15% Ni/TiO_2 (sonic) catalyst with temperature is shown in Fig. 4(a). Both the conversions increased with increasing temperature. In addition, CO_2 conversion was similar to CH_4 conversion, which indicates that the contribution of reverse water gas shift reaction ($CO_2 + H_2 \leftrightarrow CO + H_2O$) is negligible. Nearly 86% CH_4 conversion and 84% CO_2 conversion was observed at 700°C. The catalysts with the low Ni loading namely, 5% and 10% over TiO_2 were also synthesized and tested for dry reforming reaction. Both CH_4 and CO_2 conversions were found to be lower than 15% Ni/TiO_2 catalyst. At 700°C, 31% CH_4 and 34% CO_2 conversion was obtained over 5% Ni/TiO_2 catalyst while only 59% CH_4 and 56% CO_2 conversion was obtained over 10% Ni/TiO_2 catalyst.

The catalyst performance of 15% Ni/TiO_2 (imp) was also compared against the catalyst synthesized via the conventional wet impregnation method. Ni loading and amount of catalyst in both cases were kept constant. CH_4 and CO_2 conversions as a function of temperature over 15% Ni/TiO_2 (imp) are depicted in Fig. 4(c). Nearly, 64% CH_4 conversion and 72% CO_2 conversion was obtained at 700°C in the presence of the impregnated catalyst. At high temperature, the rate of reaction is controlled by diffusion of reactant. Therefore, the rate of reaction was expressed in mol $g^{-1}s^{-1}$ and the performance of both the catalysts was compared at low temperature. It was found that the reaction rates were higher for 15% Ni/TiO_2 (sonic) catalyst. Therefore, the catalyst synthesized by sonication method exhibits higher activity than the catalyst synthesized via

View Article Online
DOI: 10.1039/C3RA45961F

conventional wet impregnation. The enhancement in reforming activities of 15% Ni/TiO_2 (sonic) catalyst is due to intimate contact between Ni and TiO_2 support, as evidenced from XPS studies. It must be noted that XRD and TEM studies showed that Ni in the catalyst synthesized by sonication method had smaller crystallites size and high metal dispersion. Therefore, the enhancement in the activity of the catalyst is related to the intimate contact of Ni and TiO_2 support and fine dispersion of the active species. Further, despite an equimolar amount of CH_4 and CO_2 in the feed, CO_2 conversion was higher compared to conversion of CH_4 for the temperature range over 15% Ni/TiO_2(imp) catalyst. This indicates that the extent of occurrence of the reverse water gas shift reaction is higher over the catalyst.

The H_2/CO ratio is an important for downstream processes. Fig. 4 (b) and Fig. 4 (d) show the H_2/CO molar ratio, respectively, for 15% Ni/TiO_2 (sonic) and 15% Ni/TiO_2 (imp) catalyst at various reaction temperatures. The H_2/CO ratio increased with an increase in temperature for both the catalysts. In particular, 15% Ni/TiO_2 (sonic) catalyst reached H_2/CO ratio close to 1 above 650°C whereas 15% Ni/TiO_2 (imp) catalyst showed H_2/CO ratio lower than 1. The low value of H_2/CO ratio (<1) is due to the strong contribution of reverse water gas shift. The simultaneous occurrence of reverse water gas shift reaction consumes additional H_2 and produces extra CO, which lowers the H_2/CO ratio.

3.3 Kinetic study of steam reforming

Fig. 5(a) shows the variation of CH_4 conversion and CO selectivity with temperature over 15% Ni/TiO_2 (sonic) catalyst. Both CH_4 conversion and CO selectivity increased with increase in temperature. Nearly 92% CH_4 conversion with 77% CO selectivity was observed at 700°C. The CH_4 conversion below 400°C was small and a sharp rise in the CH_4 conversion was observed above 400°C indicating high energy barrier for this reaction. Further, at low temperature, CO

View Article Online
DOI: 10.1039/C3RA45961F

selectivity is low, which implies a large contribution from WGS reaction. The effect of steam concentration on the CO selectivity is also depicted in Fig. 5(b). The CO selectivity decreased with an increase in the inlet steam concentration due to promotion of the WGS activity.

The rate of reaction and activation energy for reforming over 15% Ni/TiO_2 (sonic) catalyst was measured by performing experiments with different amounts of catalyst loading keeping the total flow rate constant at 100 ml/min. The mixture consisting of 3% of CH_4, 3% of H_2O and balance of N_2 with the total flow rate of 100 ml/min was used. All experiments were performed under isothermal and differential conditions at atmospheric pressure over a temperature range of 450-550°C and the rate of reaction at various temperatures was calculated using following equation.

$$rate(r) = \frac{F \times x}{W} = \frac{x}{W/F} \quad (7)$$

F, W and x is flow of the gas in mol/s, weight of the catalyst in g and fractional CH_4 conversion, respectively. Fig. 6(a) shows the variation of W/F_{CO} with the fractional conversion of CH_4 at various temperatures. The plot of fractional conversion (x) with W/F_{CO} is linear up to 40% conversion and non linearity at higher CH_4 conversion indicates that the differential reactor approach is not valid at high temperature. Therefore, the rates of reaction were calculated from the slope of linear portion. The variation of rate of reaction with temperature is shown in Fig. 6(b). The apparent activation energy was calculated from the Arrhenius plot (see inset of Fig. 6 (b)) and found to be 105 kJ/mol.

The effect of concentration of CH_4, steam and CO on the rate of reaction was also investigated to understand the reaction kinetics. The rate of reaction was measured in a differential reactor in the absence of any transport artifacts under atmospheric pressure. All of the experiments were carried over 50 mg of catalyst with a total flow of 100 ml/min and reactor

View Article Online
DOI: 10.1039/C3RA45961F

temperature was varied such that the differential reactor approach (CH_4 conversion ~25%) was always maintained. The concentration of CH_4 was varied between 1 to 4 % keeping the steam concentration constant at 3.6 %. For another set of experiments, the concentration of steam was varied between 1 and 8% keeping the methane concentration constant at 3%. The effect of CO concentration on the rate of the reaction was also independently examined. The concentration of CO was varied in the range of 0.25 to 0.75%, while the inlet concentrations of CH_4 (3%) and steam (3.6%) were kept constant.

Fig. 7(a) shows the variation of rate of reaction with concentration of CH_4 at various reaction temperatures. The rate of reaction increases with the concentration of CH_4 at all temperatures. The order of reaction with respect to concentration of CH_4 was determined by plotting the variation of rate of reaction with concentration on a log-log scale. In general, the reaction is first order with CH_4 concentration for all temperatures and it is consistent with rate determining step, namely CH_4 chemisorption. Fig. 7(b) shows the variation of rate of reaction with steam concentration. A strong negative effect of steam concentration on rate of reaction was observed. This effect is attributed to an optimum concentration of steam and CH_4 coverage on the catalyst surface. The negative order of reaction with steam concentration indicates that CH_4 and steam undergo competitive adsorption on the catalyst for the same active sites. However, no maximum in the rate of reaction was observed when CH_4 concentration was varied. This observation is in line with a reaction scheme in which the rate limiting step is the activation of CH_4 molecules. The effect of inlet concentration of CO on the steam reforming is also depicted in Fig. 7(c). The rate of reaction decreases with increasing inlet concentration of CO. This effect is due to the chemisorption of CO interfering with CH_4 chemisorption on the same active surface sites. The qualitative trends presented above elucidate major mechanistic aspects of the steam

View Article Online
DOI: 10.1039/C3RA45961F

reforming reaction. Further, the measured rates reflect intrinsic kinetics without any mass transfer effects. Therefore, these observations were used to propose the reaction mechanism for steam reforming reaction.

3.4 Kinetic model

The kinetics of steam reforming has been studied extensively over noble metals (Ru, Rh, Pt) and nickel based catalysts. However, there is no agreement in the reaction mechanism and the corresponding rate expression. Several expressions including Langmuir-Hinshelwood, power laws, and expressions based on micro kinetic analysis have been proposed to describe the kinetic of reforming reaction.[6, 33] This is likely due to the different nature of the active species, identity of support, catalyst morphology (shape and size), different experimental conditions (synthesis method and testing condition etc.) and metal loading.[20] In most of the studies, the dissociative methane adsorption reaction is assumed to be a rate determining step.[8, 32] Steam and dry reforming over Ru catalyst supported on various supports have been studied and a first order kinetic equation on CH_4 concentration was proposed. No dependence on the nature of support, metal loading and concentration of H_2O or CO_2 was observed.[19, 34] The effect of various forms of support on the activity of the reaction has also been studied. Berman et al. have reported a negative reaction order in steam concentration, and speculated that the adsorption of steam occurs on Al_2O_3/MnOx support.[35] The kinetic model involving CO_2 interaction with the support was proposed for dry reforming of CH_4 over Ru/La_2O_3 catalyst.[36] On the other hand, no influence of the support on the reaction rate has also been reported.[22, 37]

The reforming reaction was studied over the nickel foil at 900°C at atmospheric pressure and the rate of reaction is satisfactory described by a simple first order equation ($rate = kP_{CH_4}$), where P_{CH_4} is the partial pressure of the CH_4 and k is the rate constant.[38] However, a simple first

View Article Online
DOI: 10.1039/C3RA45961F

order equation cannot be used to describe the kinetics of this reaction because the inlet partial pressure of H_2O has a significant influence on the rate of reaction. The high CO coverage was observed over the catalyst during the reaction.[5] The present study also showed that the negative effect of concentration of H_2O and CO on the reaction. Therefore, the development of an improved model with the effect of concentration of steam and products on the overall rate of reaction is necessary. It should be noted that the kinetic models for methane reforming are quite different from each other and depend on the experimental conditions.[20]

Based on our observations and available literature, we have proposed a set of elementary steps and the kinetic expression was derived using a Langmuir-Hinshelwood kinetic by considering the CH_4 dissociative adsorption as the rate limiting step.[39]

$$CH_4 + * \xrightarrow{K_1} C* + 2H_2 \quad (8)$$

$$H_2O + 2* \xleftrightarrow{K_2} OH* + H* \quad (9)$$

$$OH* + * \xrightarrow{k_3} O* + H* \quad (10)$$

$$C* + O* \xrightarrow{k_4} CO* \quad (11)$$

$$CO* \xleftrightarrow{k_5} CO + * \quad (12)$$

$$H* + H* \xrightarrow{k_6} H_2 + 2* \quad (13)$$

Equation (8) represents the decomposition of CH_4 into the adsorbed surface containing species (CH_3*, CH_2*, CH* and H*). The rate of hydrogen removal in subsequent steps is much higher than that of the initial C-H bond rupture. Therefore, subsequent H-abstraction from CH_4 molecules is represented by a single equation. The negative order with respect to H_2O shows that there is competitive adsorption between CH_4 and steam for the same active sites. Therefore, equation (8) and (9) assume that the activation of CH_4 and steam compete for same active sites.

View Article Online
DOI: 10.1039/C3RA45961F

The rapid steam adsorption gives the surface oxygen species (equation (10)) and the carbon species formed on the surface. This reacts rapidly with surface oxygen species resulting in product, CO (equation (11)).[40] Further, high WGS indicate that CO adsorption over the catalyst surface is considerable. The rate of reaction decreases with increasing inlet concentration of CO due to interference of CO with CH_4 chemisorption for the same surface sites (equation (12)).

The rate of reaction is first order with respect to CH_4 concentration and this implies that the dissociative adsorption of CH_4 is a rate determining step. Therefore, while deriving kinetic expression, it was explicitly assumed that the dissociative adsorption of CH_4 (equation 8) is a rate limiting step. Solving the above set of elementary steps, the following rate expression is obtained.

$$rate = \frac{K_1 C_{CH_4}}{\left(K_1 C_{CH_4} + \sqrt{K_2 C_{H_2O}} + K_5 C_{CO}\right)^2} \qquad (14)$$

The above kinetic expression is consistent with the observations that the dissociative CH_4 adsorption step, a rate determining step and activation of H_2O molecules takes place over a single metal surface atom without involvement of the support. The values of K_1, K_2 and K_5 were obtained simultaneously using non-linear regression. Fig. 8 shows the predicted rate of reaction corresponding to the experimental observed reaction rate. The model without inhibition term due to CO adsorption was also tried to fit the data but this resulted in poor fitting. Therefore, the adsorption of CO over the catalyst is substantial and cannot be ignored. The high activity of the catalyst for WGS reaction is also manifested this fact. The optimized values for K_1, K_2 and K_5 are 68 exp(-4400/T), 5400 exp(-4900/RT) and 1200 exp(-1600/RT), respectively.

View Article Online
DOI: 10.1039/C3RA45961F

Stability and deactivation studies

The dependence of catalytic activity on time on stream over 15% Ni/TiO_2 (sonic) catalyst was studied at 650° C for 16 h for both dry and steam reforming reactions. Fig. 9 (a) shows the variation of CH_4, CO_2 conversions and H_2/CO ratio over 16 h for dry reforming reaction. The stable conversion value for CH_4 and CO_2 were 65% and 67%, respectively. A small drop (about 2-3%) in both the conversions was observed for the initial few hours, which might be due to some modification of the catalyst surface causing instability in the carbon deposition.[41] However, the H_2/CO ratio (~0.96) was nearly stable over 16 h reaction period. The stability of 15% Ni/TiO_2 (imp) catalyst was also studied at 650° C for 16 h for dry reforming reaction. Fig. 9 (b) shows the variation of CH_4, CO_2 conversions and H_2/CO ratio over 16 h. The time on stream test shows that 15% Ni/TiO_2 (imp) catalyst is less stable and more than 30% loss of initial activity was observed during first 4 h of reaction. Fig. 9(c) shows the stability for steam reforming reaction. There was a slight decrease in CH_4 conversion and CO selectivity for the initial period. However, a stable CH_4 conversion (~75) and CO selectivity (~62) was observed after 4 h. Therefore, the catalyst has high activity and excellent stability for both the reactions.

TGA analysis was used to estimate the deposited coke over the catalyst. Fig. 10 shows the TGA/DTA analysis performed in the presence of pure O_2 of the spent catalyst on stream. The thermogram was divided into three different temperatures region. The first region below 260°C showed a minimal weight loss and this can be ascribed to the loss of absorbed moisture and volatile species, such as reactants and products.[42] The second region between 300°C and 600°C showed an increase in weight of the catalyst due to oxidation of the Ni particles. Finally, the third region above 600°C showed decrease in the weight of the catalyst due to oxidation of deposited coke with different degree of graphitization. The amount of coke deposited on the

View Article Online
DOI: 10.1039/C3RA45961F

spent catalyst was found to be around 0.6 wt%. The catalyst synthesized by sonochemical method showed less coke deposition due to stronger metal support interactions, contributing to good reaction stability. Meanwhile, it has been reported that relatively large Ni particles are vulnerable to coke formation.[43] Therefore, nanosized Ni particles and strong metal support interactions facilitate carbon gasification via H_2O dissociation and oxygen spillover to Ni particles.

5. Conclusions

The highly dispersed supported Ni nanoparticles over TiO_2 were successfully prepared via sonochemical assisted method and the performance of the material was investigated for dry and steam reforming of methane. The catalyst synthesized by the present approach exhibited excellent catalytic activity and stability for both the reactions than the catalyst prepared by incipient wetness impregnation method. For dry reforming, 86% CH_4 and 84% CO_2 conversion was obtained at 700°C. Nearly 92% CH_4 with 77% CO selectivity was observed at 700°C for steam reforming reaction. The high activity and stability of the catalyst is attributed to the fine dispersion (due to small metallic Ni clusters) of Ni species. The present catalyst is remarkably active and stable even after long period and no appreciable coke deposition was observed. Therefore, the present approach is a simple and feasible for the synthesis of supported metal catalyst, which can be used to enhancing the catalytic performance.

Acknowledgments

Authors gratefully acknowledge the financial support from Gas authority of India Limited.

View Article Online
DOI: 10.1039/C3RA45961F

References

1 J. Xu, C. M. Yeung, J. Ni, F. Meunier, N. Acerbi, M. Fowles and S. C. Tsang, *Appl.Catal.A.*, 2008, **345**, 119-127.

2 B. Höhlein, S. Von Andrian, T. Grube and R. Menzer, *J. Power Sources* , 2000, **86**, 243-249.

3 I. H. Son, S. J. Lee, A. Soon, H.-S. Roh and H. Lee, *Appl.Catal.B.*, 2013, **134**, 103-109.

4 H.-S. Roh, K.-W. Jun, W.-S. Dong, S.-E. Park and Y.-S. Baek, *Catal.Lett.*, 2001, **74**, 31-36.

5 J. H. Jeong, J. W. Lee, D. J. Seo, Y. Seo, W. L. Yoon, D. K. Lee and D. H. Kim, *Appl.Catal.A.*, 2006, **302**, 151-156.

6 A. Lemonidou, M. Goula and I. Vasalos, *Catal.Today.*, 1998, **46**, 175-183.

7 T. Horiuchi, K. Sakuma, T. Fukui, Y. Kubo, T. Osaki and T. Mori, *Appl.Catal.A.*, 1996, **144**, 111-120.

8 Z. Hou, O. Yokota, T. Tanaka and T. Yashima, *Catal.Lett.*, 2003, **87**, 37-42.

9 M. Halabi, M. De Croon, J. Van der Schaaf, P. Cobden and J. Schouten, *Appl. Catal. A.,* **2010**, 389, 68-79.

10 N.Laosiripojana and S. Assabumrungrat, *Appl. Catal. A.,* **2005**, 290, 200-211.

11 S. Kurungot, and T.Yamaguchi, *Catal.Lett.,* **2004**, 92, 181-187.

12 N.Laosiripojana, D. Chadwick and S. Assabumrungrat, *Chem. Eng. J.,* **2008**, 138, 264-273.

13 C. M. Kalamaras, K. C. Petallidou and A. M. Efstathiou, *Appl.Catal.B.*, 2013, 136-137, 225-238.

14 P. S. Lambrou and A. M. Efstathiou, *J.Catal.*, 2006, **240**, 182-193.

View Article Online
DOI: 10.1039/C3RA45961F

15 C. Costa, S. Christou, G. Georgiou and A. Efstathiou, *J.Catal.*, 2003, **219**, 259-272.

16 R. Duarte, M. Nachtegaal, J. Bueno and J. V. Bokhoven, *J.Catal.*, 2012, **296**, 86-98.

17 M. C. Bradford and M. A. Vannice, *Appl.Catal.A.*, 1996, **142**, 97-122.

18 N. Perkas, H. Rotter, L. Vradman, M. V. Landau and A. Gedanken, *Langmuir*, 2006, **22**, 7072-7077.

19 J. Wei and E. Iglesia, *J.Catal.*, 2004, **225**, 116-127.

20 K. O. Christensen, D. Chen, R. Lødeng and A. Holmen, *Appl.Catal.A.*, 2006, **314**, 9-22.

21 M. Goula, A. Lemonidou and A. Efstathiou, *J.Catal.*, 1996, **161**, 626-640.

22 D. Ligthart, R. Van Santen and E. Hensen, *J.Catal.*, 2011, **280**, 206-220.

23 R. A. Van Santen, *Acc. Chem. Res.*, 2008, **42**, 57-66.

24 H. S. Bengaard, J. K. Nørskov, J. Sehested, B. Clausen, L. Nielsen, A. Molenbroek and J. Rostrup-Nielsen, *J.Catal.*, 2002, **209**, 365-384.

25 L. Yin, Y. Wang, G. Pang, Y. Koltypin and A. Gedanken, *J. Colloid Interface Sci.*, 2002, **246**, 78-84.

26 Y. Wang, L. Yin and A. Gedanken, *Ultrason. Sonochem.*, 2002, **9**, 285-290.

27 P. Girault, J. Grosseau-Poussard, J. Dinhut and L. Marechal, *Nucl. Instr. Meth. Phys. Res.*, 2001, 174,439-452.

28 D. Dissanayake, M. P. Rosynek, K.C.C. Kharas and J.H. Lunsford, *J. Catal.,* 1991, **132**, 117-127.

29 Briggs D, Seah MP, Briggs D, Seah MP, (Eds), Practical surface analysis by Auger and X-ray photoelectron spectroscopy, John Wiley & Sons, Chichester, 1983.

30 I. H. Son, S. J. Lee, A. Soon, H.-S. Roh, H. Lee, *Appl. Catal. B.,*2013, **134-135**,103-109.

31 D. R. Penn, *J. Electron Spectrosc. Relat. Phenom.*, 1976, **9**, 29-40.

View Article Online
DOI: 10.1039/C3RA45961F

32 J. Scofield, *J. Electron Spectrosc. Relat. Phenom.*, 1976, **8**, 129-137

33 N. Laosiripojana and S. Assabumrungrat, *J. Power Sources.*, 2007, **163**, 943-951.

34 J. Wei and E. Iglesia, *J.Catal.*, 2004, **224**, 370-383.

35 A. Berman, R. Karn and M. Epstein, *Appl.Catal.A.*, 2005, **282**, 73-83

36 C. Carrara, J. Munera, E. Lombardo and L. Cornaglia, *Top. Catal.*, 2008, **51**, 98-106.

37 J. Wei and E. Iglesia, *J.Phy. Chem. B.*, 2004, **108**, 7253-7262.

38 M. Temkin, *Adv. Catal.*, 1979, **28**, 173-291.

39 J. G. Jakobsen, T. L. Jørgensen, I. Chorkendorff and J. Sehested, *Appl.Catal.A.*, 2010, **377**, 158-166.

40 C. A. Guimarães and M. d. Moraes, *Appl.Catal. A.*, 2004, **258**, 73-81.

41 Z. Hou and T. Yashima, *Appl.Catal. A.*, 2004, **261**, 205-209.

42 P. Djinović, I. G. Osojnik Črnivec, B. Erjavec and A. Pintar, *Appl.Catal.B.*, 2012, **125**, 259-270.

43 Y.-X. Pan, C.-J. Liu and P. Shi, *J. Power Sources.*, 2008, **176**, 46-53.

View Article Online
DOI: 10.1039/C3RA45961F

Figure captions

Fig. 1 XRD patterns of (a) 15% Ni/TiO_2 (imp) before reaction (b) 15% Ni/TiO_2 (imp) after reaction, (c) 15% Ni/TiO_2 (sonic) before reaction and (d) 15% Ni/TiO_2 (sonic) after reaction

Fig. 2 Bright field images of 15% Ni/TiO_2 (sonic) catalyst (a) as-synthesized (b) calcinated at 700^{o} C for 1 h (c) after reaction and (d) 15% Ni/TiO_2 (imp) catalyst

Fig. 3 Core level XPS of (a) Ni 2p and (b) Ti 2p.The numbers (1), (2) and (3) represent spectra for 15% Ni/TiO_2 (imp) catalyst, 15% Ni/TiO_2 (sonic) catalyst before and after the reaction, respectively

Fig. 4 Catalytic activity for the dry reforming (a) CH_4 conversion and CO_2 conversion (b) H_2/CO ratio as a function of temperature for 15% Ni/TiO_2 (sonic) catalyst and (c) CH_4 conversion and CO_2 conversion (d) H_2/CO ratio as a function of temperature for 15% Ni/TiO_2 (imp) catalyst

Fig. 5 Variation of (a) CH_4 conversion and (b) CO selectivity with H_2O/CH_4 ratio at various temperature over 15% Ni/TiO_2 (sonic) catalyst for steam reforming reaction

Fig. 6 (a) Variation of fractional conversion of CH_4 with W/F_{CH4} and (b) rate of reaction as function of temperature for steam reforming reaction over 15% Ni/TiO_2 (sonic) catalyst

Fig. 7 (a) The effect of concentration of CH_4 on the rate of methane conversion at a constant steam concentration of 2.7% (b) effect of H_2O concentration on the rate of methane conversion

View Article Online
DOI: 10.1039/C3RA45961F

at a constant methane concentration of 3% (c) effect of CO concentration on the rate of methane conversion at constant methane (3%) and steam concentration (2.7%), respectively

Fig. 8 Comparison between experimentally measured rate and calculated rate from the model for steam reforming reaction

Fig. 9 Time on steam (a) CH_4, CO_2 conversion and H_2/CO ratio for dry reforming of methane over 15 % Ni/TiO_2 (sonic) catalyst, (b) CH_4, CO_2 conversion and H_2/CO ratio for dry reforming of methane over 15 % Ni/TiO_2 (imp) catalyst and (c) CH_4 conversion and CO selectivity for steam reforming reaction over 15 % Ni/TiO_2 (sonic) catalyst

Fig. 10 TGA-DTA plot for the catalyst under pure oxygen after on stream in steam reforming reaction over 15 % Ni/TiO_2 (sonic) catalyst

View Article Online
DOI: 10.1039/C3RA45961F

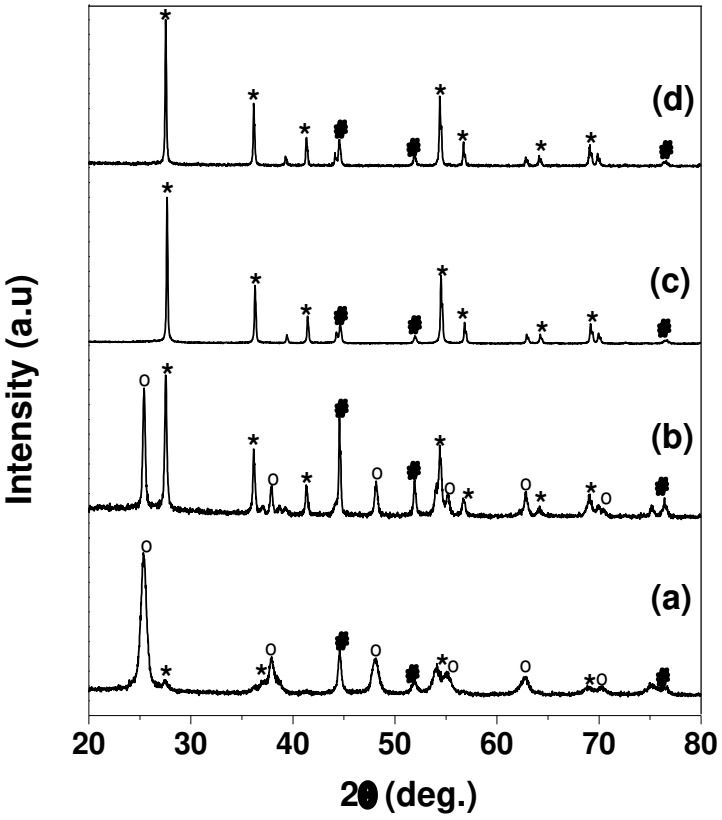

Fig. 1 XRD patterns of (a) 15% Ni/TiO_2 (imp) before reaction (b) 15% Ni/TiO_2 (imp) after reaction, (c) 15% Ni/TiO_2 (sonic) before reaction and (d) 15% Ni/TiO_2 (sonic) after reaction (o-anatase, *-rutile and #- Ni metal)

View Article Online
DOI: 10.1039/C3RA45961F

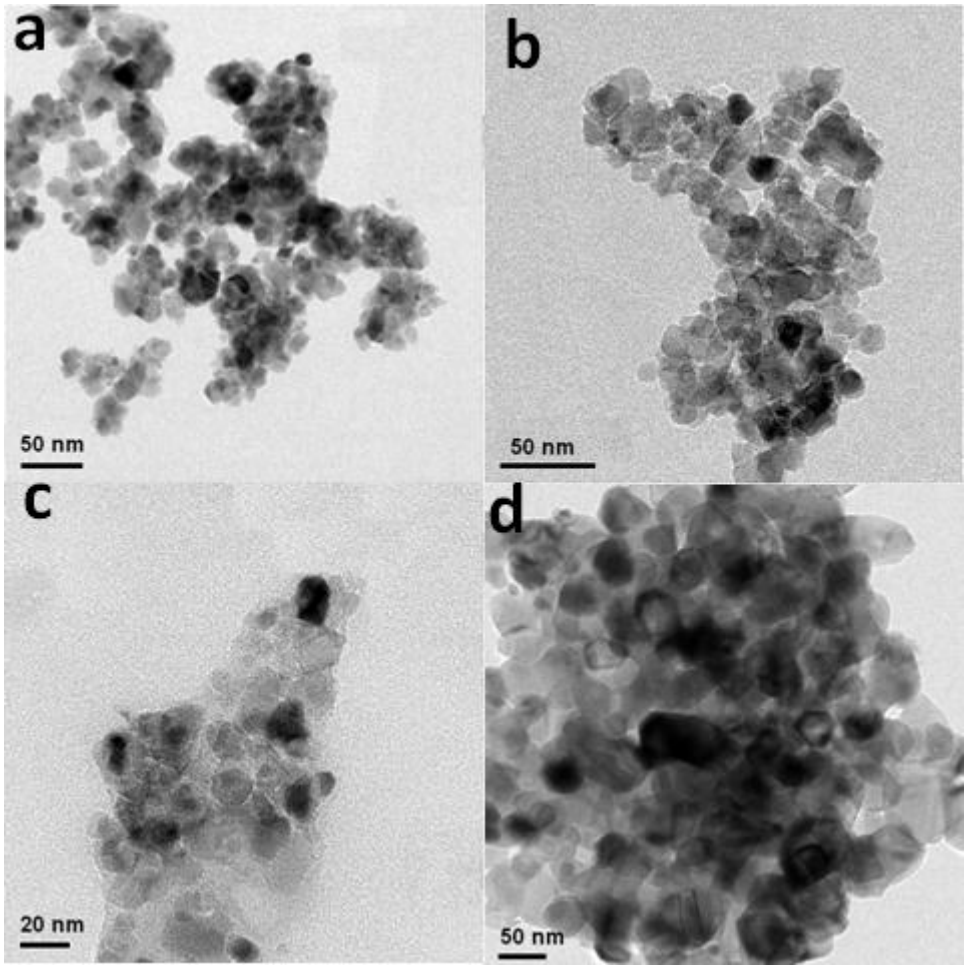

Fig. 2 Bright field images of 15% Ni/TiO_2 (sonic) catalyst (a) as-synthesized (b) calcinated at 700° C for 1 h (c) after reaction and (d) 15% Ni/TiO_2 (imp) catalyst

View Article Online
DOI: 10.1039/C3RA45961F

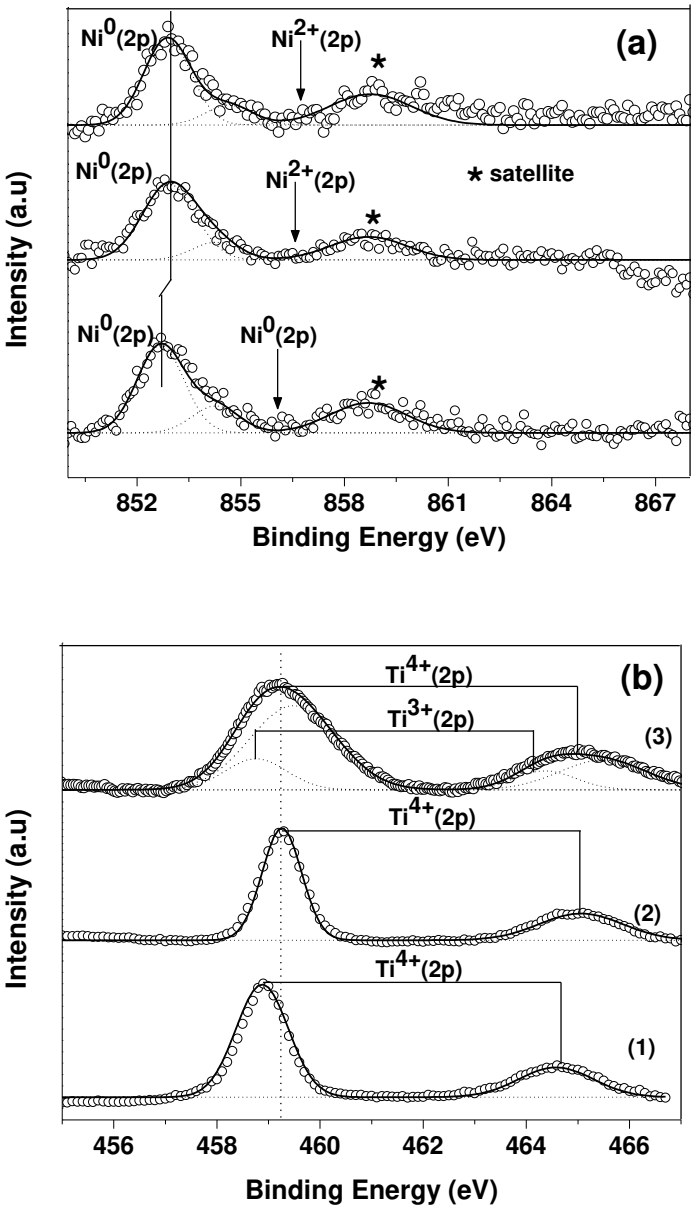

Fig. 3 Core level XPS of (a) Ni 2p and (b) Ti 2p.The numbers (1), (2) and (3) represent spectra for 15% Ni/TiO_2 (imp) catalyst, 15% Ni/TiO_2 (sonic) catalyst before and after the reaction, respectively

View Article Online
DOI: 10.1039/C3RA45961F

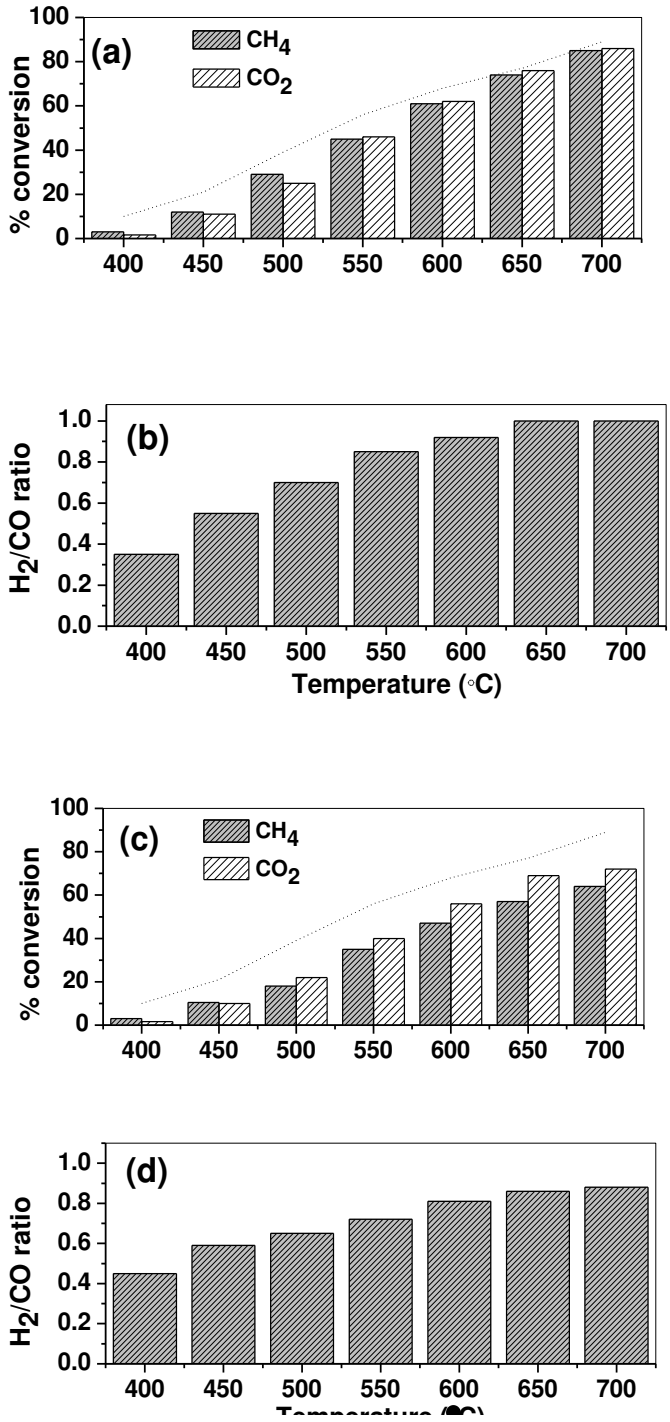

Fig. 4 Catalytic activity for the dry reforming (a) CH_4 conversion and CO_2 conversion (b) H_2/CO ratio as a function of temperature for 15% Ni/TiO_2 (sonic) catalyst and (c) CH_4 conversion and CO_2 conversion (d) H_2/CO ratio as a function of temperature for 15% Ni/TiO_2 (imp) catalyst

View Article Online
DOI: 10.1039/C3RA45961F

(Gas composition: 2% CH_4, 2% CO_2 and balance N_2 with total gas flow 100 ml/min, over 75 mg of catalyst. Dotted line represents the equilibrium conversion)

View Article Online
DOI: 10.1039/C3RA45961F

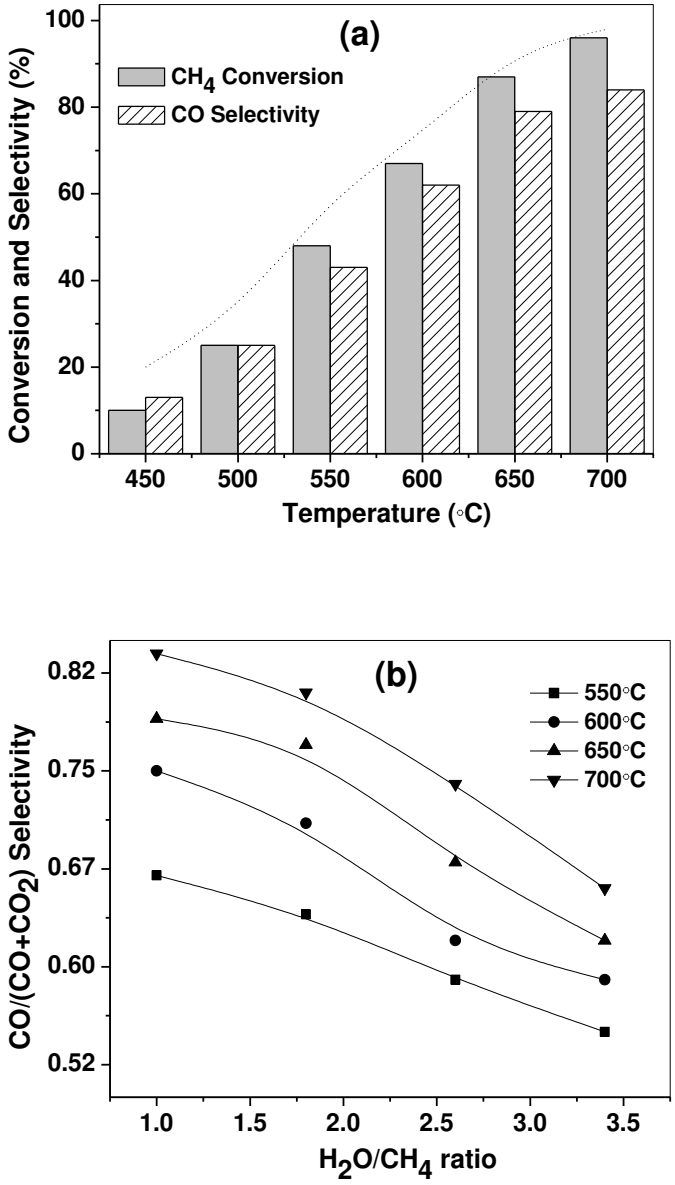

Fig. 5 Variation of (a) CH_4 conversion and (b) CO selectivity with H_2O/CH_4 ratio at various temperature over 15% Ni/TiO_2 (sonic) catalyst for steam reforming reaction (Gas composition: 3% CH_4 and balance N_2 with total gas flow 100 ml/min, over 150 mg of 15% Ni/TiO_2 (sonic) catalyst. Dotted line represents the equilibrium conversion)

View Article Online
DOI: 10.1039/C3RA45961F

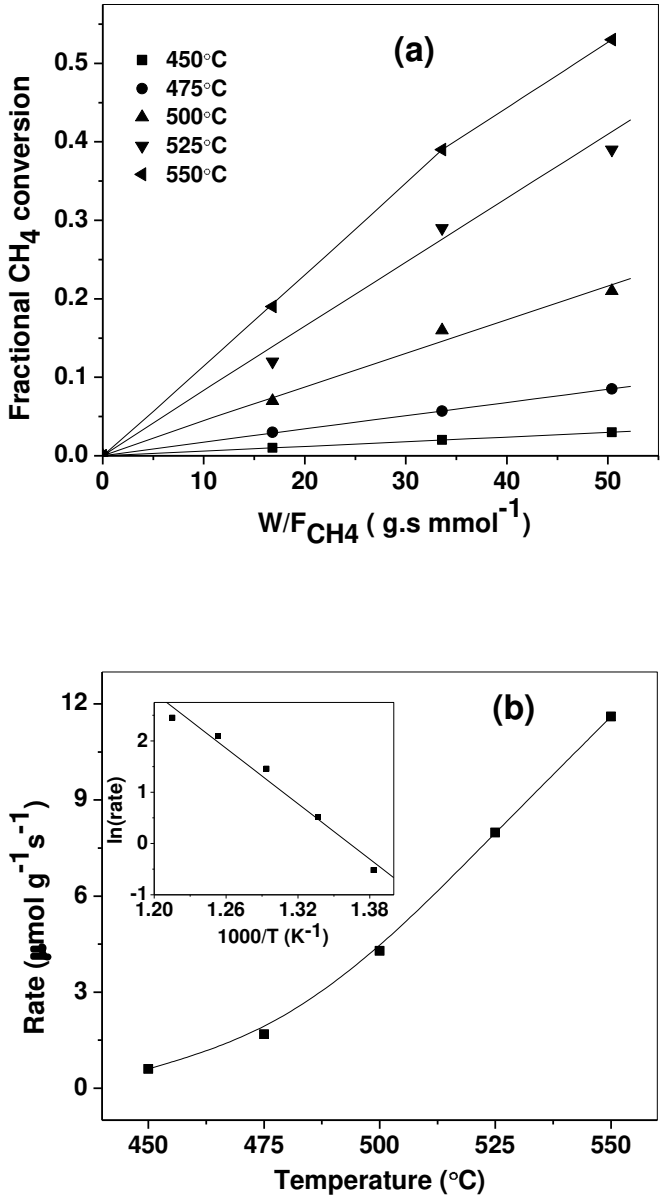

Fig. 6 (a) Variation of fractional conversion of CH_4 with W/F_{CH4} and (b) rate of reaction as function of temperature for steam reforming reaction 15% Ni/TiO_2 (sonic) catalyst

View Article Online
DOI: 10.1039/C3RA45961F

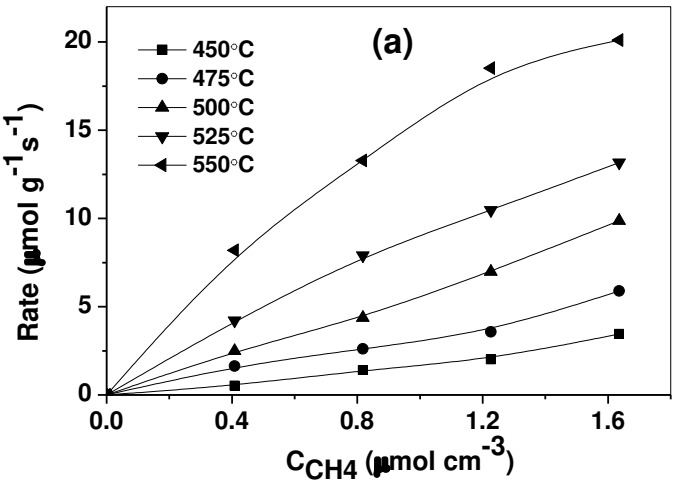

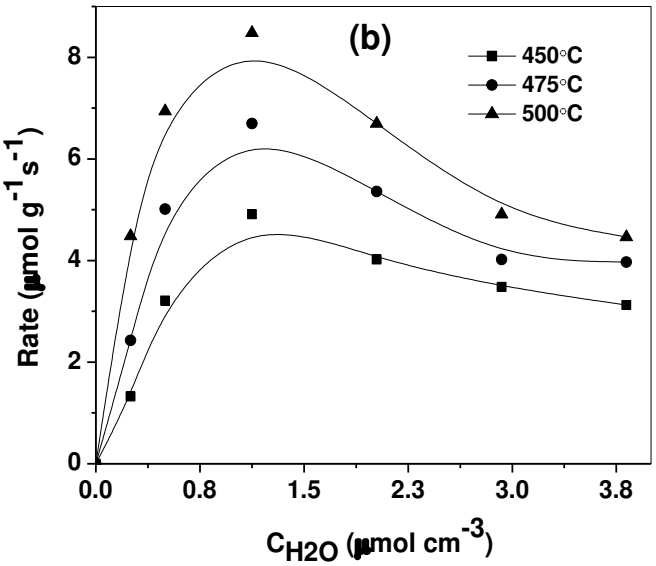

View Article Online
DOI: 10.1039/C3RA45961F

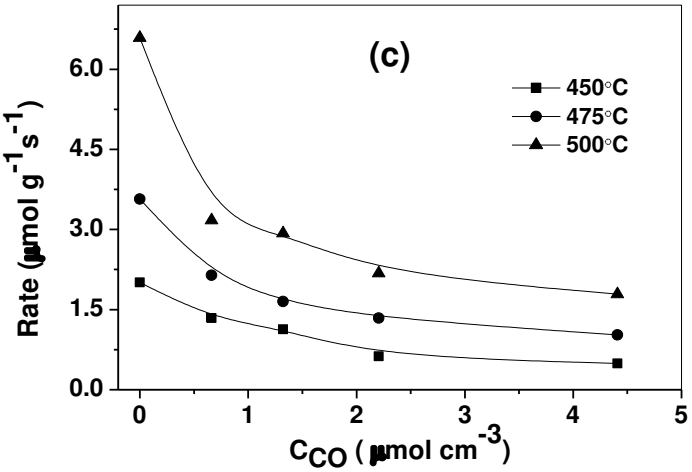

Fig. 7 (a) The effect of concentration of CH_4 on the rate of methane conversion at a constant steam concentration of 3.6% (b) effect of H_2O concentration on the rate of methane conversion at a constant methane concentration of 3% (c) effect of CO concentration on the rate of methane conversion at constant methane (3%) and steam concentration (3.6%), respectively

View Article Online
DOI: 10.1039/C3RA45961F

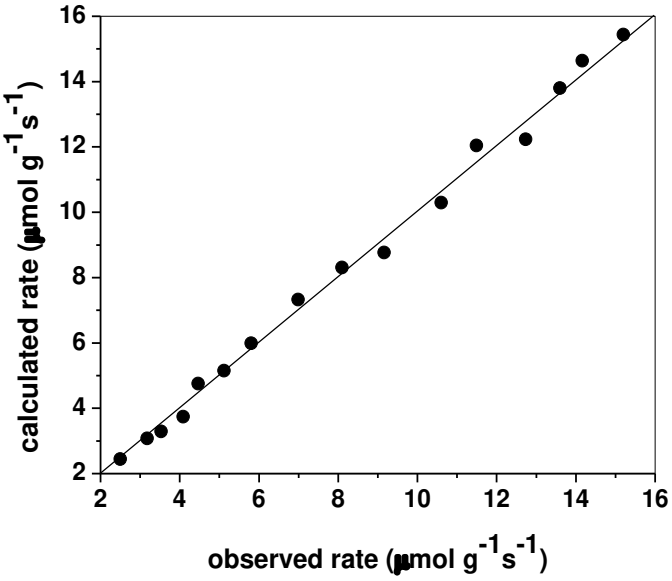

Fig. 8 Comparison between experimentally measured rate and calculated rate from the model for steam reforming reaction

View Article Online
DOI: 10.1039/C3RA45961F

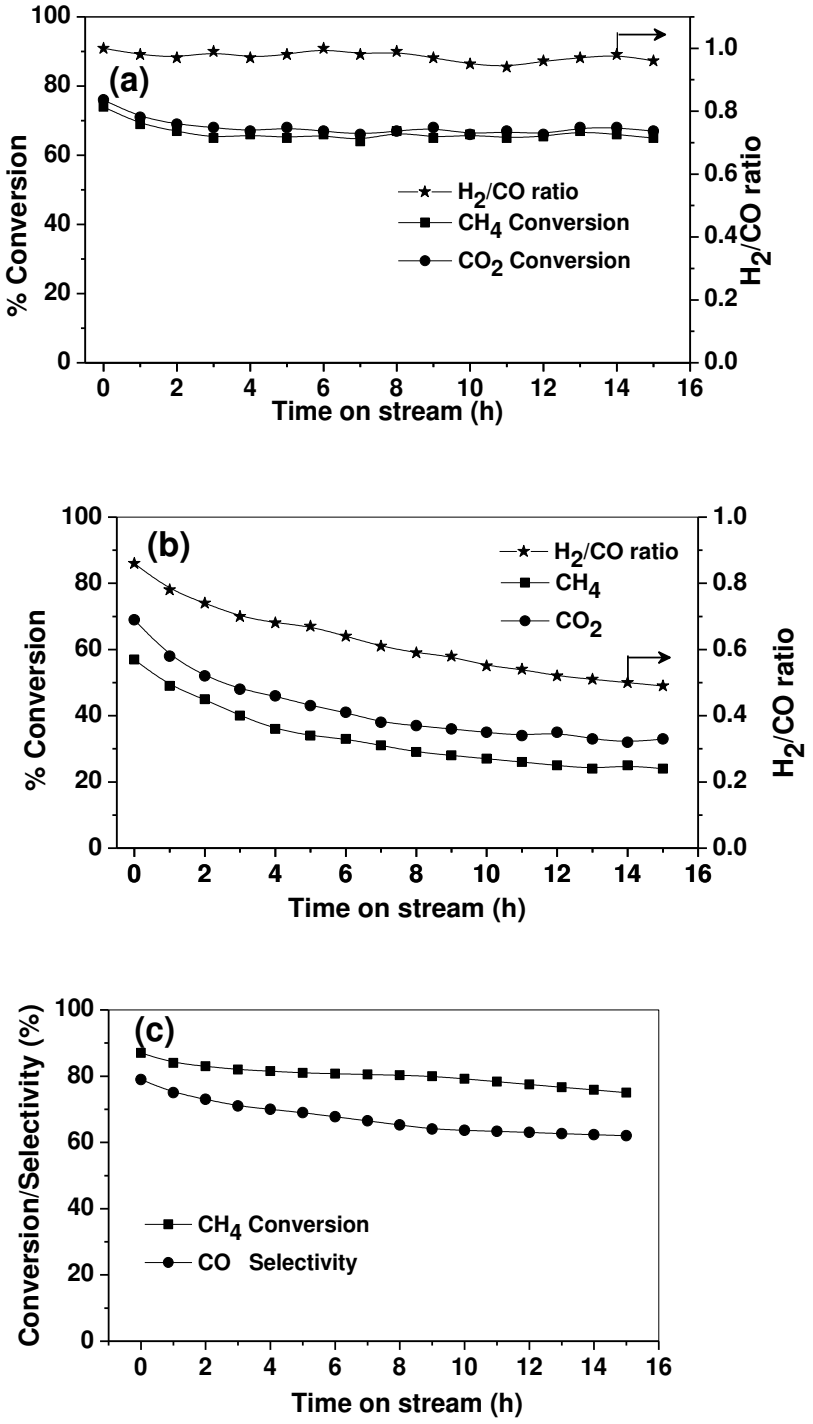

Fig. 9 Time on steam (a) CH_4, CO_2 conversion and H_2/CO ratio for dry reforming of methane over 15 % Ni/TiO_2 (sonic) catalyst, (b) CH_4, CO_2 conversion and H_2/CO ratio for dry reforming of methane over 15 % Ni/TiO_2 (imp) catalyst and (c) CH_4 conversion and CO selectivity for

View Article Online
DOI: 10.1039/C3RA45961F

steam reforming reaction over 15 % Ni/TiO_2 (sonic) catalyst (Reaction conditions for dry reforming: 2% CH_4, 2% CO_2 and balance N_2 with total gas flow 100 ml/min over 75 mg of catalyst and reaction conditions for steam reforming: 3% CH_4 (H_2O/CH_4 ratio=1.2) and balance N_2 with total gas flow 100 ml/min over 150 mg of catalyst)

View Article Online
DOI: 10.1039/C3RA45961F

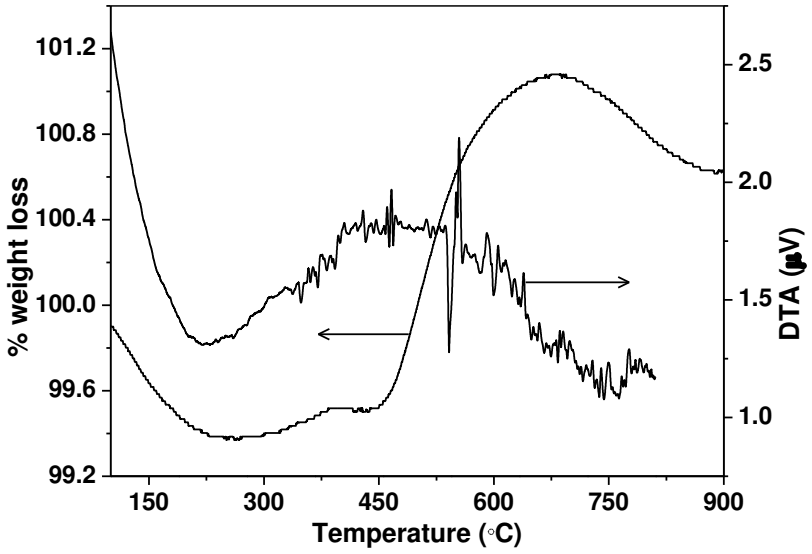

Fig. 10 TGA-DTA plot for the catalyst under pure oxygen after on stream in steam reforming reaction over 15 % Ni/TiO_2 (sonic) catalyst